International Journal of Electrical, Electronic and Communication Sciences
ISSN: 2517-9438
Vol:2, No:6, 2008

Wavelet based ANN Approach for Transformer Protection

Okan Özgönenel

Abstract**—**This paper presents the development of a wavelet based algorithm, for distinguishing between magnetizing inrush currents and power system fault currents, which is quite adequate, reliable, fast and computationally efficient tool. The proposed technique consists of a preprocessing unit based on discrete wavelet transform (DWT) in combination with an artificial neural network (ANN) for detecting and classifying fault currents. The DWT acts as an extractor of distinctive features in the input signals at the relay location. This information is then fed into an ANN for classifying fault and magnetizing inrush conditions. A 220/55/55 V, 50Hz laboratory transformer connected to a 380 V power system were simulated using ATP-EMTP. The DWT was implemented by using Matlab and Coiflet mother wavelet was used to analyze primary currents and generate training data. The simulated results presented clearly show that the proposed technique can accurately discriminate between magnetizing inrush and fault currents in transformer protection.

Keywords**—**Artificial neural network, discrete wavelet transform, fault detection, magnetizing inrush current.

I. Introduction

POWER transformers are important devices in the power system. Reliability and stability of the whole power system are the primary issues concerning transformers. Transformer relaying protection of automation system is critical for the safe operation of transformers. Therefore, the continuity of transformer operation is of vital importance in maintaining the reliability of power supply. Any unscheduled repair work, especially replacement of a faulty transformer is very expensive and time consuming [1].

Traditionally, the current differential technique based on power frequency measurements offers satisfactory overall performance. The protection demands during exciting inrush the protection system should be reliably disabled, which is a problem for existing current differential technique, because it introduces significant unbalanced current and the protection will surely response without inrush detection. The correct and effective identification between faults and exciting inrush remains a challenge for protection deployment [2].

Under transformer internal and external faults, the three-phase current is mainly sinusoidal, except for some DC element and harmonics. However, under exciting inrush, the transformer response is featured by singular eruptions composed of high-frequency elements because of the non-linearity of exciting core. It is possible to make use of this high-frequency eruption information to achieve satisfactory detection performance [3].

O. Özgönenel is with Department of Electrical and Electronic Engineering, Ondokuz Mayis University, Kurupelit, 55139, Samsun, Turkey (e-mail: okanoz@omu.edu.tr).

Three kinds of schemes are currently used for this purpose. Some schemes make use of the information obtained only from the incoming currents of the transformer, such as the method based on the second harmonics restraint principle. Some schemes make use of the information obtained from the variation of the transformer terminal voltages, such as the method based on the voltage restraint principle. Other alternative schemes make use of the information obtained from both the currents and voltages of the transformers, such as the method based on the flux characteristic principle and the method based on the Low-Voltage acceleration criterion. However, the most widely used method in practice is still those which are based on the principle of the second harmonic restraint. The main drawback of this kind of method is that the harmonics existed in the long EHV transmission lines will cause the differential relay either not to operate or to operate with a long-time delay [4], [5].

Nevertheless, the current transformer's (CT's) saturation is an obstacle to the application of this scheme in the digital differential protection. Therefore, it is of importance to search a new scheme which can discriminate the inrush current and short circuit faster and more reliability.

Differential algorithms such as discrete Fourier transform, least-square method, rectangular transforms, walsh functions and haar functions, etc. are used to calculate the current harmonic contents. The main drawbacks of this approach are that the second harmonic may also exist in some internal faults within transformer windings, and the new low-loss amorphous core materials in modern power transformers may produce lower 2^{nd} harmonic content in the current. The mainly involving transformer inductance during saturation, artificial neural networks, fuzzy logic, etc. these approaches are dependent on the transformer parameters [6], [7].

Wavelet transform (WT), as a milestone of the development of the Fourier transform, has attracted great attention and been successfully used in many applications in the past decade. Its application in the power system is also under investigation in the recent years. The application in power systems includes analysis and detection of electromagnetic transients, power quality assessment, data compression, and fault detection [8], [9].

This paper proposed a new wavelet based ANN method to identify inrush currents and to distinguish it from power system faults. The proposed algorithm extracts fault and inrush generated transient signals using DWT. The extracted information from transient signals are simultaneously in both time and frequency domains. In this study, Coiflet 6 wavelets are used to construct first level filter bank to extract the transients. In this paper, discontinuities in the current samples are mainly in the scope of the proposed algorithm. The output signal of the DWT module is then fed into a feed-forward,

back-propagation ANN that classifies the transient. The DWT considerably simplifies the input signal of the ANN; it reduces the volume of the input data of the ANN without lost of information. This dramatically reduces the training stage in the ANN and increases the overall performance of the digital relay. The construction of ANN has three inputs, a hidden layer with two neurons, and eight output neurons in the output layer. Extensive simulation studies have been conducted to verify the feasibility of proposed protection scheme under variety of energizing conditions with different source triggering angles, winding connections, and fault conditions with symmetrical and unsymmetrical faults.

The next section aims to introduce wavelet transform into the power system protective relaying with the emphasis on the transformer inrush identification.

II. Principle of WT

Since Morlet first began to use wavelet analysis, it has been widely studied by many mathematicians, physicist, engineers, etc. today, its interest is spread out on not only theoretical but various applied fields, for example, speech or image signal processing, vibration analysis and so on. The wavelet analysis need not to use a single window function in all frequency components, or has linear resolution in the whole frequency domain that are weakpoints for Fourier analysis. There is enough reason that much interest concentrates on wavelet in time-frequency analysis [10].

Wavelet analysis provides a basis for $L^2(R)$ and in many wavelet systems the elements of this basis are orthogonal to each other and normalized. Wavelet analysis providing a basis for $L^2(R)$ is similar to the set $\{\cos(n\omega_0 t), \sin(n\omega_0 t) : n \in Z\}$ forming an orthogonal basis for periodic functions having frequency ω_0. Using a wavelet expansion, any function in $L^2(R)$ can be expressed as a sum of the basis elements

$$f(t) = \sum_{k=-\infty}^{\infty} c_k \varphi(t-k) + \sum_{k=-\infty}^{\infty} \sum_{j=0}^{\infty} d_{j,k} 2^{j/2} \psi(2^j t - k) \qquad (1)$$

Parameter j determines the scale or the frequency range of each wavelet basis function ψ. Parameter k determines the time translations. The defining characteristic of a wavelet or multi-resolution system is that $\psi(t)$ satisfies a scaling equation such as

$$\varphi(t) = \sum_{k=-\infty}^{\infty} h[k] \sqrt{2} \varphi(2t-k) \qquad (2)$$

for some sequence $h[k]$ that is usually finite. The wavelet function $\psi(t)$ is derived from $\varphi(t)$. Each coefficient can be calculated as the inner product between $f(t)$ and the respective basis element. The L^2 inner products and alternative notation for the coefficients in (1) are

$$\begin{aligned} c[k] \equiv c_k &= \int_{-\infty}^{\infty} f(t) \varphi(t-k) dt \\ d_j[k] \equiv d_{j,k} &= \int_{-\infty}^{\infty} f(t) 2^{j/2} \psi(2^j t - k) dt \end{aligned} \qquad (3)$$

The $c[k]$ are called approximation coefficients and the $d_j[k]$ are called detail coefficients. The approximation coefficients together are comparable to the null harmonic (DC) value in a Fourier expansion. The Haar wavelet system is the earliest and simplest. Its basis elements are translated and scaled versions of the following functions:

$$\begin{aligned} &\varphi(t) = 1 \quad \text{for } t \in (0,1) \text{ and } \varphi(t) = 0, \text{ otherwise.} \\ &\psi(t) = 1 \quad \text{for } t \in (0,0.5) \\ &\psi(t) = -1 \quad \text{for } t \in (0.5,1) \text{ and } \psi(t) = 0, \text{ otherwise.} \end{aligned} \qquad (4)$$

The wavelet function $\psi(t)$ is somewhat similar to one period of $\sin(2\pi t)$. At a particular j the translates $\psi(2^j t - k)$ line up right next to each without overlapping for $k \in Z$ [11], [12].

The wavelet function is localized in time and frequency yielding wavelet coefficients at different scales (levels). This gives the WT much greater compact support for the analysis of signals with localized transient components. The DWT output can be represented in a two-dimensional (2D) grid in a similar manner as the short time Fourier transformation (STFT), but with very different divisions in time and frequency, such that the windows are narrow at high frequencies and wide at low frequencies. In contrast with the STFT, the WT can isolate transient components in the upper frequency isolated in a shorter part of power frequency cycle. In discrete wavelet analysis of a signal, a time-frequency picture of the analyzed signal is set up. The time-frequency plane is a 2D space useful for idealizing a two properties of transient signals, localization in time of transient phenomena, and presence of specific frequencies. The signal is decomposed into segments called time-frequency tiles plotted on the plane. The position of the tiles indicates the nominal time, while the amplitude is indicated by shading. As shown in Fig. 1, two sinusoids with 50Hz, 50Hz + 150Hz + 250Hz + 350Hz, and a sampling rate 2kHz, are plotted below. This corresponds to 40 samples per cycle. 2 kHz is chosen in order to capture the high frequency components of the signals.

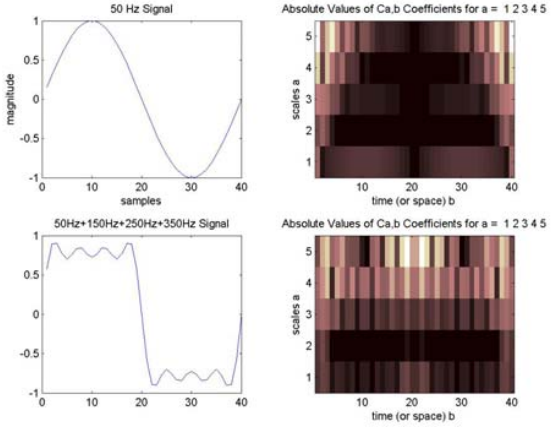

Fig. 1 Sinusoidal signals and their time-frequency tiles

In Fig. 1, time-frequency tiles are obtained by using Morlet wavelet with the level of 5. The DWT is represented by the time-frequency tiles, and the mother wavelet function is dilated at low frequencies (level – 5) and compressed at high frequencies (level – 1) so that large windows are used to obtain the low frequency components of the signal, while small windows reflects discontinuities.

Coiflet wavelets are designed for the purpose of maintaining a close match between the trend values and the original signal values. Following a suggestion of Coifman, these wavelets first constructed by Daubechies, who called them "coiflets". All of the coiflet wavelets are defined in a similar way; so this paper shall concentrate on the simplest case of Coif6 wavelets [13], [14]. The scaling numbers for the Coif6 scaling signals are listed below:

$$\alpha_1 = \frac{1-\sqrt{7}}{16\sqrt{2}}, \alpha_2 = \frac{5+\sqrt{7}}{16\sqrt{2}}, \alpha_3 = \frac{14+2\sqrt{7}}{16\sqrt{2}}, \alpha_4 = \frac{14-2\sqrt{7}}{16\sqrt{2}},$$
$$\alpha_5 = \frac{1-\sqrt{7}}{16\sqrt{2}}, \alpha_6 = \frac{-3+\sqrt{7}}{16\sqrt{2}}$$

Using these scaling numbers, the first level Coif6 scaling signals defined by

$$\begin{aligned} V_1^1 &= (\alpha_1,\alpha_2,\alpha_3,\alpha_4,\alpha_5,\alpha_6,0,0....) \\ V_2^1 &= (0,0,\alpha_1,\alpha_2,\alpha_3,\alpha_4,\alpha_5,\alpha_6,0,0....) \\ V_3^1 &= (0,0,0,0,\alpha_1,\alpha_2,\alpha_3,\alpha_4,\alpha_5,\alpha_6,0,0....) \\ &.. \\ &.. \\ V_{\frac{N}{2}-1}^1 &= (0,0,0,....\alpha_1,\alpha_2,\alpha_3,\alpha_4,\alpha_5,\alpha_6,0,0) \\ V_{\frac{N}{2}}^1 &= (\alpha_3,\alpha_4,\alpha_5,\alpha_6,0,....0,0,\alpha_1,\alpha_2,0,0) \end{aligned} \quad (5)$$

where N is the number of samples.

As a generalized expression, (5) can be re-written as:

$$V_m^1 = \alpha_1 V_{2m-1}^0 + \alpha_2 V_{2m}^0 + \alpha_3 V_{2m+1}^0 + \alpha_4 V_{2m+2}^0 + \alpha_5 V_{2m+3}^0 + \alpha_6 V_{2m+4}^0 \quad (6)$$

The Coif6 wavelet numbers are defined by β1 = α6, β2 = -α5, β3 = α4, β4 = -α3, β5 = α2, β6 = -α1 and these wavelet numbers determine the first – level Coif6 wavelets as follows:

$$\begin{aligned} W_1^1 &= (\beta_1,\beta_2,\beta_3,\beta_4,\beta_5,\beta_6,0,0....) \\ W_2^1 &= (0,0,\beta_1,\beta_2,\beta_3,\beta_4,\beta_5,\beta_6,0,0....) \\ W_3^1 &= (0,0,0,0,\beta_1,\beta_2,\beta_3,\beta_4,\beta_5,\beta_6,0,....) \\ &.. \\ &.. \\ W_{\frac{N}{2}-1}^1 &= (0,0,0,....\beta_1,\beta_2,\beta_3,\beta_4,\beta_5,\beta_6,0,0) \\ W_{\frac{N}{2}}^1 &= (\beta_3,\beta_4,\beta_5,\beta_6,0,....0,0,\beta_1,\beta_2) \end{aligned} \quad (7)$$

As a generalized expression, (7) can be re-written as:

$$W_m^1 = \beta_1 V_{2m-1}^0 + \beta_2 V_{2m}^0 + \beta_3 V_{2m+1}^0 + \beta_4 V_{2m+2}^0 + \beta_5 V_{2m+3}^0 + \beta_6 V_{2m+4}^0 \quad (8)$$

Inverse wavelet transform for Coif6 is expressed as:

$$F = A^1 + D^1 \quad (9)$$

In (9), A is called the *approximation* and D is called the *detail* signal where F is the synthesized signal.

At level 1, A is defined as

$$A^1 = (F.V_1^1)V_1^1 + (F.V_2^1)V_2^1 + ... + (F.V_{N/2}^1)V_{N/2}^1 \quad (10)$$

At level 1, D is defined as

$$D^1 = (\mathrm{F.W}_1^1)W_1^1 + (\mathrm{F.W}_2^1)W_2^1 + ... + (\mathrm{F.W}_{\mathrm{N/2}}^1)W_{N/2}^1 \quad (11)$$

Inverse wavelet transform for Coif6 at level 2 is expressed as

$$F = A^2 + D^2 + D^1 \quad (12)$$

At level 2, A is defined as:

$$A^2 = (F.V_1^2)V_1^2 + ... + (F.V_{N/4}^2)V_{N/4}^2 \quad (13)$$

At level 2, D is defined as:

$$D^2 = (F.W_1^2)W_1^2 + ... + (F.W_{N/4}^2)W_{N/4}^2 \quad (14)$$

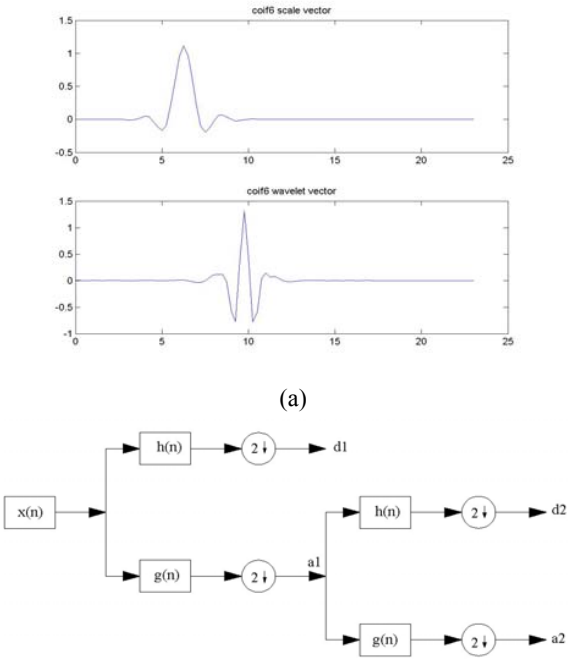

Fig. 2 (a) Coif6 wavelet and scale function, (b) wavelet decomposition tree

III. Back-Propagation Neural Network

Neural network have been trained to perform complex functions in various fields of application including pattern recognition, identification, classification, speech, vision and control systems. The most widely used neural network is back-propagation. Back-propagation attempts to minimize error by adjusting each value of a network proportional to the derivative of error with respect to that value. This is called gradient descent. In the back-propagation learning, the actual outputs are compared with the target values to derive the error signals, which are propagated backward layer by layer for the updating of the synaptic weights in all the lower layers.

One of the most critical problems in constructing the ANN is the choice of the number of hidden layers and the number of neurons for each layer. Using too few neurons in the hidden layer may prevent the training process to converge, while using too many neurons would produce long training time, and/or result in the ANN to lose its generalization attribute. In this paper, a number of tests were performed varying with the one or two hidden layers as well as varying the number of neurons in each hidden layer with full connections between the neurons. A hidden layer with two neurons was assumed adequate for classifying eight outputs. Total iteration number was set to 2000.

To discriminate inrush current and short circuit current, the typical three layer architecture are used as follows: it has one input layer with three neurons, a hidden layer with two neurons and an output layer with eight neurons. Hidden layer has sigmoidal neurons which receive inputs directly and then broadcast their outputs to a layer of linear neurons which compute the network output.

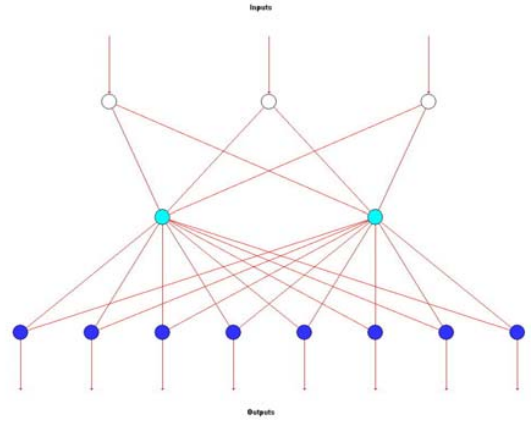

Fig. 3 A feed-forward, back-propagation ANN structure

This architecture has been proven capable of approximating any function with a finite number of discontinuities with arbitrary accuracy. It is used to discriminate inrush current and short-circuit current here.

Number of neurons has been optimized by neglecting very low coefficients. The input data of the ANN is organized in a sliding-window of a quarter of cycle (5ms, 10 samples of primary and secondary currents). The DWT splits the signal in details and broad signals, each with 10 coefficients. The ANNs are fed with the three detail signals; thus, the input vector has 30 elements. The detection ANN has eight output neurons which indicate the existence of magnetizing inrush, normal operating condition, phase to phase fault, two phase to ground fault, three phase short circuit fault, phase to phase fault, overload condition and circuit breaker operating. All the output neurons have binary decisions such as 1 and 0. in case of a fault condition and overload condition the output neuron of circuit breaker is set to 1 otherwise 0.

In Fig. 4, the three phase transformer is connected in star-ground/star-ground and fault begins at 200ms and ends at 240ms with a fault resistance of 1Ω. To simulate high impedance faults, different values of fault resistances were selected and analyzed.

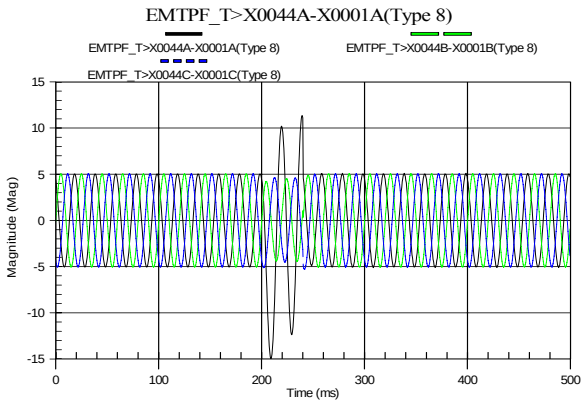

Fig. 4 Single phase to ground fault on secondary side

A total of 300 simulations were generated, half of them were used for training, and the other half for testing. The

current signal of the faulty phase, the detail and the broad signal are displayed on Fig. 5.

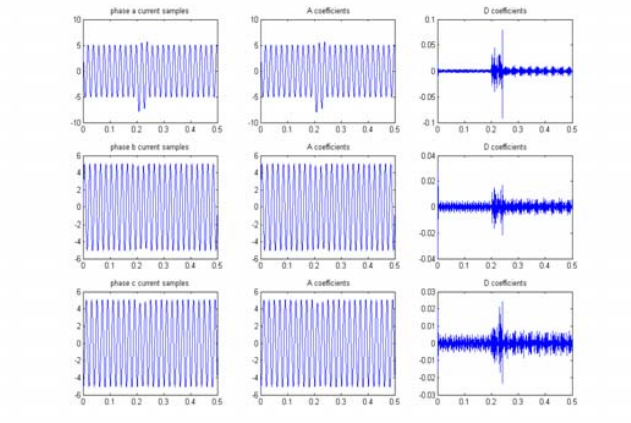

Fig. 5 Single phase to ground fault and wavelet decompositions

In Fig. 5, the left column represents secondary phase current on rated load, the middle column represents A coefficients while the right one represents D coefficients. As seen from the D coefficients of the faulty phase, the magnitudes of the spikes are higher than the others. In this case, the simulation continues 0.5 second. The DFT solution of the fault current gives only fundamental harmonic component (3.6A, 50 Hz), but it can be observed the detail signal (D) clearly shows distinctive features of the transients, i.e., immediately after the fault occurrence several sharp spikes appear in the detail signal indicating the occurrence of a fault. For all simulations, the step length of the moving window is ¼ cycle (5ms at 50Hz) and sampling frequency is 2kHz.

In a similar way, Fig. 6 and Fig. 7 show the simulations of magnetizing inrush and normal operating condition on rated load, respectively, and their DWT solutions.

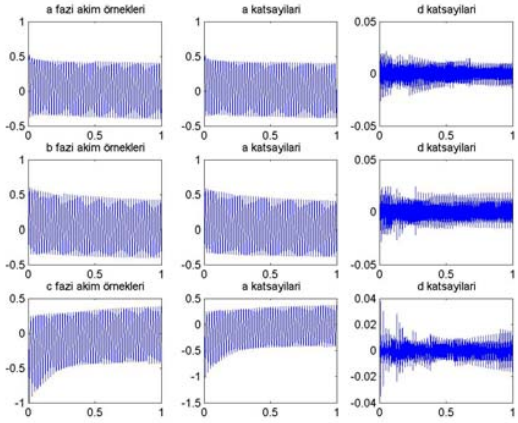

Fig. 6 Magnetizing inrush condition and variation of D coefficients

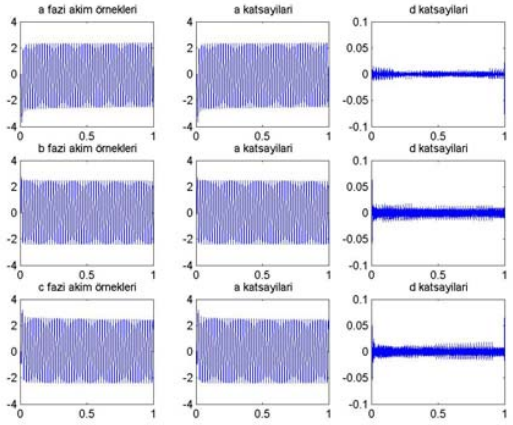

Fig. 7 Normal operating condition on rated load and variation of D coefficients

The overall fault detection flowchart diagram is shown in Fig. 8. Transformer currents are obtained through CTs and sampled by NI- Data Acquisition Card (16 Bits) with a sample frequency of 2000 Hz. Acquired current samples are sliding-windowed for discrete wavelet transform. Wavelet transform at level 1 with Coif 6 is processed at the next stage. Obtained data is prepared for neural network computation with 3 inputs and 8 outputs. If inrush current is detected, the relay is restraint and, otherwise, in case of internal fault detection, the relay sends a trip signal immediately.

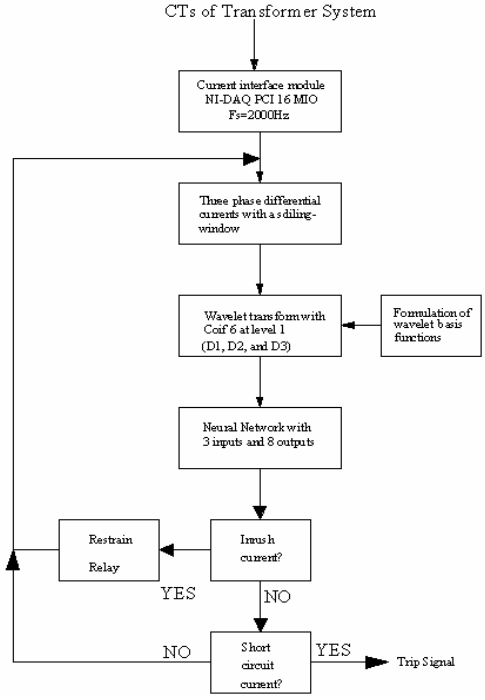

Fig. 8 The overall fault detection flowchart

IV. Response Evaluation

In this section, the ANN responses will be seen from tables. The input is a set of D1, D2, and D3 of inrush current or short-circuit current of each phases using discrete wavelet

TABLE I
TRAINING VALUES DURING MAGNETIZING INRUSH

D1	D2	D3	mag	normal	pg	ppg	tp	pp	ol	cb
0	0	0	1.0	1.0	0	0	0	0	0	0
0	0	0	1.0	1.0	0	0	0	0	0	0
0	0	0	1.0	1.0	0	0	0	0	0	0
0	0	0	1.0	1.0	0	0	0	0	0	0
-0.0001	0.0006	-0.0005	1.0	1.0	0	0	0	0	0	0
-0.0003	0.0018	-0.0015	1.0	1.0	0	0	0	0	0	0
0.0004	-0.0022	0.0018	1.0	1.0	0	0	0	0	0	0
0.0021	-0.0116	0.0095	1.0	1.0	0	0	0	0	0	0
-0.0006	0.0032	-0.0026	1.0	1.0	0	0	0	0	0	0
-0.0079	0.0432	-0.0354	1.0	1.0	0	0	0	0	0	0

TABLE II
THE ANN RESPONSE AFTER 2000 ITERATION FOR MAGNETIZING INRUSH CONDITION

T	C	T	C	T	C	T	C	T	C	T
1.0	1.000017	1.0	1.000026	0.0	0.000021	0.0	0.000022	0.0	0.000024	1.0
1.0	1.000017	1.0	1.000026	0.0	0.000021	0.0	0.000022	0.0	0.000024	1.0
1.0	1.000017	1.0	1.000026	0.0	0.000021	0.0	0.000022	0.0	0.000024	1.0
1.0	1.000017	1.0	1.000026	0.0	0.000021	0.0	0.000022	0.0	0.000024	1.0
1.0	1.000057	1.0	1.000052	0.0	0.000057	0.0	0.000051	0.0	0.000058	1.0
1.0	1.000135	1.0	1.000106	0.0	0.000127	0.0	0.000108	0.0	0.000126	1.0
1.0	0.999860	1.0	0.999920	0.0	-0.000120	0.0	-0.00009	0.0	-0.00011	1.0
1.0	0.999196	1.0	0.999470	0.0	-0.000719	0.0	-0.00057	0.0	-0.00068	1.0
1.0	1.000253	1.0	1.000185	0.0	0.000234	0.0	0.000194	0.0	0.000228	1.0
1.0	1.003160	1.0	1.002145	0.0	0.002851	0.0	0.002309	0.0	0.002742	1.0

transform. In Table I, transformer is switched on at 0.5ms after the simulation starts, therefore the four values of D1, D2, and D3 are zero. Since magnetizing inrush is assumed as normal operation, the output neurons of mag and normal are set to 1, while the others 0.

In Table I;
The output neuron "mag" refers to "magnetizing inrush condition",
The output neuron "normal" refers to "normal operating condition",
The output neuron "pg" refers to "single phase to ground fault",
The output neuron "ppg" refers to "two phase to ground fault",
The output neuron "tp" refers to "three phase short-circuit",
The output neuron "pp" refers to "phase to phase fault",
The output neuron "ol" refers to "over-load condition", and
The output neuron "cb" refers to "circuit breaker position".

In Table II, T refers to target value and C refers to ANN response.

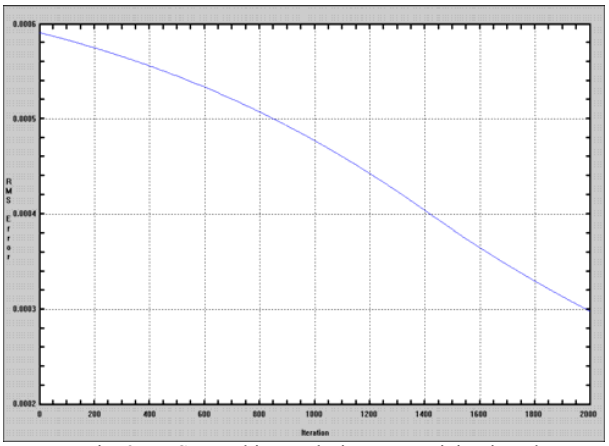

Fig. 9 RMS error history during magnetizing inrush

Fig. 9 shows the RMS network error when using back-propagation neural network training. Training is ended when the RMS error reaches the value of 0.0003.

Network Statistics during training stage for the case of magnetizing inrush can be summarized as below:

Network Name: mag
Iterations: 2000

TRAINING DATA: mag1.txt

Node	Std. Dev	Bias	Max Error	Correlation
mag.	0.00031	7.0244e-06	0.00076	0.0000e+00
normal	0.00041	1.0478e-05	0.00101	0.0000e+00
pg	0.00034	9.4074e-06	0.00084	2.8612e-05
ppg	0.00031	1.1909e-05	0.00077	1.9501e-05
tp	0.00041	1.0126e-05	0.00100	3.0889e-05
pp	0.00046	1.2509e-05	0.00112	3.3033e-05
OL	0.00043	1.0733e-05	0.00107	2.6865e-05
cb	0.00064	1.2544e-05	0.00157	3.0736e-05

Network Statistics during testing stage for the case of magnetizing inrush can be summarized as below:

Network Name: mag

RECALL DATA: mag1_test.txt

Node	Std Dev	Bias	Max Error	Correlation
mag	0.00022	-3.6681e-05	0.00066	0.0
normal	0.00086	-0.00018	0.00260	0.0
pg	0.00092	-0.00020	0.00277	0.0
ppg	0.00217	-0.00050	0.00657	0.0
tp	0.00073	-0.00015	0.00221	0.0
pp	0.00130	-0.00029	0.00392	0.0
over_load	0.00075	-0.00016	0.00226	0.0
cb	7.6618e-05	1.3982e-05	0.00019	0.0

As stated in Section I, approximately 170 series of simulations are performed to see the performance of the proposed algorithm during magnetizing inrush.

TABLE III
THE ANN RESPONSE AFTER 2000 ITERATION FOR SINGLE PHASE TO GROUND FAULT IN TRAINING STAGE

Pg (T)	Pg (C)	Cb (T)	Cb (C)
1.0	0.999011	1.0	0.999072
1.0	0.998445	1.0	0.998582
1.0	1.002006	1.0	1.001838
1.0	0.999448	1.0	0.999483
1.0	0.999689	1.0	0.999715
1.0	1.000136	1.0	1.000127
1.0	0.999624	1.0	0.999633
1.0	1.001861	1.0	1.001806
1.0	0.998737	1.0	0.998774
1.0	0.997940	1.0	0.997990

In Table III, Pg (T) refers to target value of phase to ground fault neuron, Pg (C) refers to calculated value of phase to ground fault neuron, Cb (T) refers to target value of circuit breaker operating neuron, and Cb (C) refers to calculated value of circuit breaker operating neuron. Since this proposed method works in a quarter cycle, only ten samples are shown in Table III. In this case study, the laboratory transformer is connected inYnYn0 and R phase to ground fault occurs between the time 0.2s and 0.23s in secondary side.

In testing stage, the laboratory transformer is connected in YnD5 and single phase to ground fault occurs in S phase. The proposed algorithm easily detects single phase to ground fault and sets the circuit breaker condition 1 in ¼ cycle (5ms) as seen below:

```
mag    =  -0.00013
normal =  -0.00019
pg     =   0.99979  (defective phase)
ppg    =  -0.00016
tp     =  -0.00016
pp     =  -0.00017
ol     =  -0.00018
cb     =   0.99981  (circuit breaker operation)
```

Approximately 100 series of studies involving many practically encountered different system and fault condition have shown that the protection technique based on a combined DWT and ANN is very effective in accurately discriminating between magnetizing inrush and short-circuit faults. It is apparent that an ANN with three layers with two neurons in hidden layer, when combined with DWT, gives the best performance.

The following example gives the performans results of the proposed algorithm under the 35% overload condition for the model transformer.

Network Statistics during testing stage for the case of overload condition can be summarized as below:

Network Name: overload

RECALL DATA: overload_test.txt

Node	Std Dev	Bias	Max Error	Correlation
1	0.00027	6.6204e-05	0.00079	0.0
2	0.00021	3.8196e-05	0.00059	0.0
3	0.00030	8.9594e-05	0.00065	0.0
4	0.00027	4.5546e-05	0.00076	0.0
5	0.00029	8.4952e-05	0.00058	0.0
6	0.00019	4.6949e-05	0.00054	0.0
7	0.00031	9.0182e-05	0.00083	0.0
8	0.00031	8.8906e-05	0.00077	0.0

Targets and network outputs for the case of overloaded transformer are shown at below:

Network Name: overload

		Target	Calculated
Output Node 1	(target,output) =	0.0	0.00004
Output Node 2	(target,output) =	0.0	-0.00011
Output Node 3	(target,output) =	0.0	0.00043
Output Node 4	(target,output) =	0.0	-0.00017
Output Node 5	(target,output) =	0.0	0.00045
Output Node 6	(target,output) =	0.0	0.00003
Output Node 7	(target,output) =	1.0	1.00027
Output Node 8	(target,output) =	1.0	1.00033

As stated before; output node 7 refers to OL (overload) and output node 8 refers to cb (circuit breaker operating condition) and proposed algorithm easily detects overload condition and sends a trip signal.

V. Conclusion

This paper presents a novel technique for distinguishing between inrush currents and short-circuit currents in transformer systems by combining wavelet transform and neural network technique. The ability of wavelets to decompose the signal into frequency bands in both time and frequency allows accurate fault detection. Since this method is used for discontinuity analysis of the signals, even if the fault occurs at the lowest time space with high impedance at the fault location, detail coefficients of the signal give us faulty condition. The required calculations are very simple, it is only necessary to perform a wavelet decomposition at level 1 for Coif 6. The proposed wavelet has proved optimal performance within tested faults.

The ANN correctly classifies the fault with advantages in accuracy and speed upon classical algorithms. A faster response is obtained since only a quarter of cycle from the occurrence of the fault is required. The performance shown demonstrates that the proposed technique gives a very high accuracy in classification of the transients ($\approx 99\%$). The proposed technique can be used as an attractive and effective approach for alternative protection algorithm for large power transformers.

References

[1] Zhonghao Yang and et all, "A New Technique For Power Transformer Protection Using Discrete Dyadic Wavelet Transform", Development in Power System Protection, Conference Publication No. 479, IEE, 2001.

[2] F. Jiang and et all, "Power Transformer Protection Based On Transient Detection Using Discrete Wavelet Transform (WT)", Power Engineering Society Winter Meeting, 2000. IEEE , Volume:3,23-27Jan.2000 Page(s): 1856 -1861 Vol.. 3.

[3] Xiangning Lin, Pei Liu, Shijie Cheng, "A Wavelet Based Scheme For Power Transformer Inrush Identification", Power Engineering Society Winter Meeting, 2000. IEEE , Volume: 3 , 23-27 Jan. 2000 Page(s): 1862 -1867 Vol.. 3

[4] Shaohua Jiao, Wanshun Liu, Peipu Su, Qixun Yang, Zhenhua Zhang; Jianfei Liu; "A New Principle of Discriminating Between Inrush Current and Internal Short Circuit of Transformer Based on Fuzzy Sets", Power System Technology, 1998. Proceedings. POWERCON '98. 1998 International Conference on , Volume: 2 , 18-21 Aug. 1998 Page(s): 1086 -1090 vol. 2.

[5] Saleh, S.A., Rahman, M.A**., "**Off-line Testing of a Aavelet Packet-based Algorithm for Discriminating Inrush Current in Three-phase Power Transformers", Power Engineering, 2003 Large Engineering Systems Conference on , 7-9 May 2003, Page(s): 38 -42.

[6] Saleh A. Saleh and M.A. Rahman, "Transient Model of Power Transformer Using Wavelet Fitler Bank", Proceedings of The 2002 Large Engineering Systems Conference on Power Engineering, 2002 IEEE, 0-7803-7520-3.

[7] Qi Li, David, Chan Tat Wai, "Investigation of Transformer Inrush Current Using A Dyadic Wavelet", IEEE Catalogue No: 98EX137, 0-7803-4495-2/98.

[8] Harumi Kamada, Nobuharu Aoshima, "Analog Gabor Transform Fitler with Complex First Order System", SICE, 97, July 29-31, Tokushima.

[9] Yong Sheng, Steven M. Rovnyak, "Decision Trees and Wavelet Analysis for Power Transformer Protection", Power Delivery, IEEE Transactions on , Volume: 17 Issue: 2 , April 2002, Page(s): 429 -433.

[10] Omar A.S. Youssef, "A Wavelet-Based Technique for Discrimination Between Faults and Magnetizing Inrush Currents in Transformer", IEEE Transactions on Power Delivery, Vol. 18, No. 1, January, 2003.

[11] Karen L. Buttler-Purry, Mustafa Bagriyanik, "Characterization of Transients in Transformers Using Discrete Wavelet Transforms", IEEE Transactions on Power Delivery, Vol. 18, No. 2, May, 2003.

[12] Moises Gomez-Morante, Denise W. Nicoletti, "A Wavelet Based Differential Transformer Protection", IEEE Transactions on Power Delivery, Vol. 14, No. 4, October, 1999.

[13] Sng Yeow Hong, Wang Qin, "A Wavelet Based Method to Discriminate Between Inrush Current and Internal Fault", Power System Technology, 2000. Proceedings. PowerCon 2000. International Conference on , Volume: 2 , 4-7 Dec. 2000, Page(s): 927 -931 vol. 2

[14] Peilin L. Mao, Raj K. Aggarwal, "A Novel Approach to the Classification of the Transient Phenomena in Power Transformers Using Combined Wavelet Transform and Neural Network", IEEE Transactions on Power Delivery, Vol. 16, No. 4, October, 2002.

Okan Ozgonenel was born in Samsun, Turkey. He received M.Sc degree in electrical education from Marmara University in 1992, Ph.D degree in electrical engineering from Sakarya University in 2001. He has been with Ondokuz Mayis University since 1991 where he is a lecturer at Electrical & Electronics Engineering Department. His main research interests are digital algorithms, digital signal processing, simulation methods for power transformers, power system control and protection, and wavelet techniques.